iScience

Article

Rapgef3 modulates macrophage reprogramming and exacerbates synovitis and osteoarthritis under excessive mechanical loading

Graphical abstract

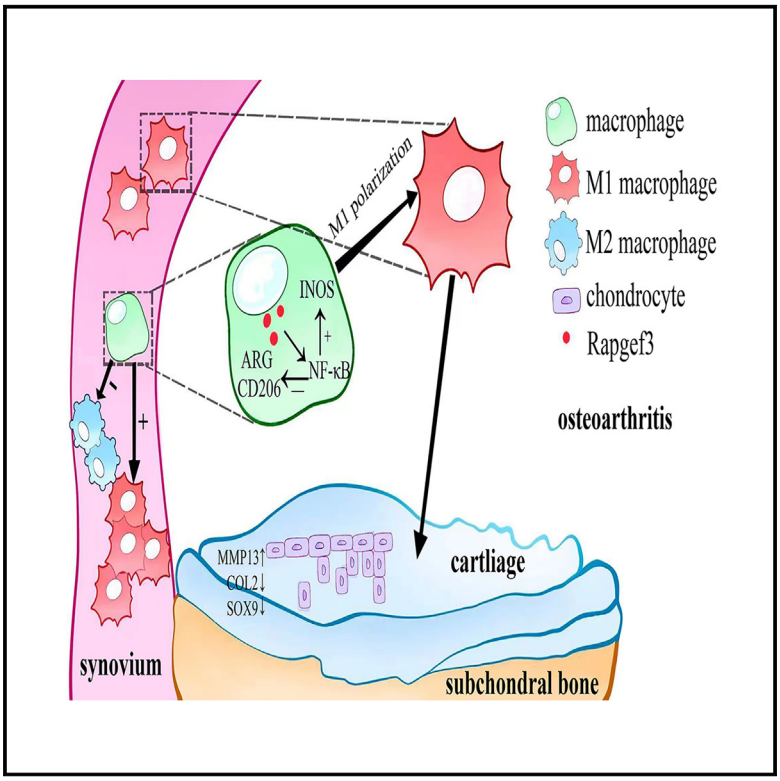

Highlights

- Investigated the relationship of mechanical stress, synovial macrophages, and OA
- Rapgef3 promoted the inflammation of macrophage, resulting in articular cartilage injury
- Experimental validation of Rapgef3 *in vivo* and *in vitro*

Authors

Wen Tang, Jian-bin Yin, Ren-gui Lin, ..., Liang-liang Liu, Yan-li Liu, Hai-yan Zhang

Correspondence

liuliangliang67@163.com (L.-l.L.), yanliliu1116@163.com (Y.-l.L.), zhhy0704@126.com (H.-y.Z.)

In brief

Biological sciences; Molecular biology; Immunology; Biomechanics; Transcriptomics

Tang et al., 2025, iScience *28*, 112131
May 16, 2025
https://doi.org/10.1016/j.isci.2025.112131

CellPress

iScience

CellPress
OPEN ACCESS

Article

Rapgef3 modulates macrophage reprogramming and exacerbates synovitis and osteoarthritis under excessive mechanical loading

Wen Tang,[1,2,3,4,5] Jian-bin Yin,[1,2,3,4,5] Ren-gui Lin,[1,2,3,4,5] Chun-yu Wu,[1,2,3,4] Jia-luo Huang,[1,2,3,4] Jin-jian Zhu,[1,2,3,4] Ling-feng Yang,[1,2,3,4] Guang-ming Li,[1,2,3,4] Dao-zhang Cai,[1,2,3,4] Liang-liang Liu,[1,2,3,4,*] Yan-li Liu,[3,4,*] and Hai-yan Zhang[1,2,3,4,6,*]

[1]Department of Joint Surgery, Center for Orthopaedic Surgery, The Third Affiliated Hospital of Southern Medical University, Guangzhou, China

[2]Department of Orthopedics, Orthopedic Hospital of Guangdong Province, Academy of Orthopedics·Guangdong Province, The Third Affiliated Hospital of Southern Medical University, Guangzhou, China

[3]The Third School of Clinical Medicine, Southern Medical University, Guangzhou, China

[4]Guangdong Provincial Key Laboratory of Bone and Joint Degeneration Diseases, Guangzhou, China

[5]These authors contributed equally

[6]Lead contact

*Correspondence: liuliangliang67@163.com (L.-l.L.), yanliliu1116@163.com (Y.-l.L.), zhhy0704@126.com (H.-y.Z.)

https://doi.org/10.1016/j.isci.2025.112131

SUMMARY

Evidence indicates that mechanical loading plays an important role in osteoarthritis (OA) progression, while the specific pathological changes of the synovium under excessive mechanical loading are unclear. Results showed that excessive mechanical loading caused pro-inflammation of synovial macrophages, which has been confirmed to exist in OA. High Rapgef3 expression level was found in RNA sequencing of RAW246.7 subjected to 0.5 Hz and 20% cyclic tensile strain. We verified this in the synovium of patients with OA and destabilization of the medial meniscus (DMM)-OA mice. Interestingly, the Rapgef3 content of chondrocytes was very low. Primary chondrocytes treated with Rapgef3 alone did not show metabolic phenotype, but an OA phenotype appeared when treated with Rapgef3-stimulated macrophage culture supernatant. Mechanically, excessive mechanical loading activated p65-nuclear factor κB (NF-κB) pathway through Rapgef3, which promoted the inflammation of macrophage, resulting in severe articular cartilage injury. Intra-articular Rapgef3 knockout reversed synovitis and cartilage degeneration, which might provide a therapeutic target for OA.

INTRODUCTION

Osteoarthritis (OA) is a chronic and highly prevalent joint disease that frequently affects the knee and hip joints.[1] Its development is associated with many factors, including sex, weight, age, and excessive stress.[2–4] Common clinical features of OA are articular cartilage destruction, joint space narrowing, synovitis, subchondral osteosclerosis, and osteophyte formation.[5] With OA occurrence and development, the patient gradually loses motor function and even becomes disabled, affecting the quality of life. OA treatment brings serious economic burden to the country and individuals.[6]

Appropriate mechanical stress has a vital impact on joint health and maintenance, but excessive mechanical loading can lead to articular cartilage degeneration and further OA development.[7,8] In recent decades, OA has been recognized as a mechanical force-related problem in clinical practice, and in most patients with OA, the knee joint axis is asymmetrical, resulting in various deformities and uneven force distribution. This, in turn, leads to synovial hyperplasia and severe cartilage wear within the joint, further accelerating OA progression.[9,10] In our previous studies, we exposed chondrocytes to loading durations of 6, 12, or 24 h, respectively. Interestingly, our findings revealed that the application of a 24-h loading period resulted in detrimental effects on chondrocyte viability.[11] However, the specific effect of excessive mechanical loading on joint synovial cells has not been elucidated.

Recent studies have shown that synovitis increased the risk of OA. It triggers pannus and osteoclast formation, enhances synovial tissue adhesion to cartilage, and leads to the release of inflammatory mediators. Intra-articular inflammation can cause articular cartilage destruction and further exacerbate the OA process.[12,13] Synovial macrophages play an important role in synovitis and OA.[14] Macrophages are plastic cells that can be divided into activated pro-inflammatory macrophages and reactivated anti-inflammatory macrophages. Pro-inflammatory macrophages produce a large number of pro-inflammatory mediators, including interleukin (IL)-1, IL-6, IL-12, tumor necrosis factor

alpha, and cyclooxygenase-2. Conversely, anti-inflammatory macrophages exhibit anti-inflammatory effects and secrete IL-4 and IL-10, contributing to tissue repair and reconstruction.[14,15] The imbalance of pro-inflammatory/anti-inflammatory macrophages can indicate the severity of knee OA.[16,17] Experiments have shown that pro-inflammatory macrophages intensified experimental collagenase-induced OA, whereas anti-inflammatory macrophages reduced OA development.[18] However, OA pathogenesis is not fully understood.

In this study, we found that excessive mechanical loading stimulated pro-inflammatory macrophages in cultured Raw246.7 cells and identified Rapgef3. Rapgef3 is a cyclic AMP (cAMP-1)-activated exchange protein, also known as a new sensor of cAMP, widely expressed and involved in many cell growth processes (cell proliferation, migration, and adhesion).[19–21] In retinal research, the absence of Rapgef3 can significantly reduce vascular inflammation.[22] Rapgef3 is involved in diseases such as atherosclerosis, Alzheimer's disease, and retinal neurodegeneration and also plays an important role in migration, proliferation, and apoptosis in several types of cancer.[22–24] We observed that Rapgef3 exhibited the highest stability among the top 10 upregulated proteins in RAW246.7 and bone-marrow-derived macrophages (BMDMs) subjected to 0.5 Hz and 20% cyclic tensile strain loading, which was also increased in the synovium of patients with OA and destabilization of the medial meniscus (DMM)-OA mice. In summary, we speculated that there is a correlation between Rapgef3 and OA caused by excessive mechanical loading. Because there is currently no research on the role of Rapgef3 in OA, we decided to investigate its potential participation. Additionally, Rapgef3 activates the nuclear factor κB (NF-κB) pathway of osteoclasts and induces osteoclast differentiation.[25] Moreover, we found significantly increased activation of the Rapgef3 and NF-κB pathways in OA and that NF-κB pathway activation promoted synovial macrophage inflammatory. Pro-inflammatory macrophages secrete inflammatory factors that act on chondrocytes, affecting their anabolism and further exacerbating OA. Furthermore, we reversed this process by knocking down Rapgef3 in synovial macrophages. In addition, we investigated an "excessive mechanical loading-macrophage-chondrocyte" model, through which we can better understand OA pathogenesis and development and identify new targets to investigate OA treatment.

RESULTS

Increased macrophage Rapgef3 expression under excessive mechanical loading and in OA synovium

To investigate the effect of mechanical loading on macrophage differentiation, RAW264.7 cells were treated using 0.5 Hz and 5%, 10%, and 20% cyclic tensile strain loading for 8, 16, and 24 h. The 0.5 Hz and 5% cyclic tensile strain loading treatment for 24 h could down-regulate INOS and CD80 (pro-inflammatory macrophage marker) but upregulated CD206 and ARG1 (anti-inflammatory macrophage marker) mRNA levels, indicating that macrophages exhibited anti-inflammatory functions under low mechanical load. In contrast, 10% and 20% cyclic tensile strain for 24 h enhanced pro-inflammatory macrophages; anti-inflammatory macrophages were significantly inhibited at 20% cyclic tensile strain (Figures 1A and S1A). To understand the mechanism of enhanced pro-inflammatory macrophages under mechanical loading, we conducted RNA sequencing on three 0.5 Hz and 0% cyclic tensile strain and three 0.5 Hz and 20% cyclic tensile strain for 24 h loading-treated RAW264.7 cells. On the basis of the sequencing results, we repeatedly detected the top 10 genes with upregulated expression in the Raw246.7 cells and BMDMs treated with 0.5 Hz and 20% cyclic tensile strain load for 24 h and found that Rapgef3 was stably and significantly upregulated in pro-inflammatory macrophages induced by excessive mechanical loading (Figures 1B–1D and S1C–S1F). Through the analysis of Kyoto Encyclopedia of Genes and Genomes pathway enrichment map of the sequencing results, we found that the related pathway of RA rheumatoid arthritis changed significantly after stretching, suggesting that stretched macrophages may be related to joint inflammation, so Rapgef3 is a potential target (Figure S1B).

To investigate Rapgef3 expression in OA synovium, synovial tissues were obtained from patients with OA and DMM-OA mice. Immunohistochemistry (IHC) showed a significant increase in Rapgef3 in human OA synovial tissue (Figure 1E). Additionally, immunofluorescence staining revealed that Rapgef3 was significantly increased in synovial macrophages of DMM-OA mice (Figure 1F).

These findings suggested that excessive mechanical loading led to pro-inflammation of macrophages with increased Rapgef3, which was closely associated with OA progression.

Rapgef3 enhances pro-inflammatory of macrophages and inhibition of Rapgef3 reduces pro-inflammatory

To evaluate the effects of Rapgef3 on macrophages, RAW246.7 cells and BMDMs were transfected with different Rapgef3 concentrations with a Rapgef3-overexpression plasmid. Rapgef3 was found to be significantly overexpressed in RAW264.7 cells and BMDMs treated with 3 μg/mL plasmid, which enhanced pro-inflammation and inhibited anti-inflammation of macrophages (Figures 2A–2D and S2A–S2D). Subsequently, Rapgef3 was knocked down in RAW246.7 cells and BMDMs by transfection with Rapgef3 small interference RNA (siRNA). The results showed that Rapgef3 knockdown inhibited macrophage pro-inflammatory direction, but had no significant effect on anti-inflammatory (Figures 2E, 2F, S2E, and S2F). Interestingly, upon Rapgef3 knockdown in 0.5 Hz and 20% cyclic tensile strain load-treated RAW246.7 cells, the enhancement of pro-inflammatory direction induced by excessive mechanical loading was significantly inhibited, whereas the inhibited anti-inflammatory direction was reversed (Figures 2G, 2H, S2G, and S2H). These results suggested that Rapgef3 enhanced pro-inflammation and inhibited anti-inflammation of macrophages, while Rapgef3 knockdown alleviated the pro-inflammatory/anti-inflammatory imbalance caused by excessive mechanical loading.

Rapgef3 has no direct effect on chondrocytes

Subsequently, we investigated Rapgef3 expression and function on chondrocytes. Interestingly, the results of IHC showed that Rapgef3 was significantly increased in synovial macrophages of DMM-OA mice but was barely expressed on articular cartilage (Figure 3A). To determine whether Rapgef3 had an effect on chondrocytes, primary mouse chondrocytes were transfected

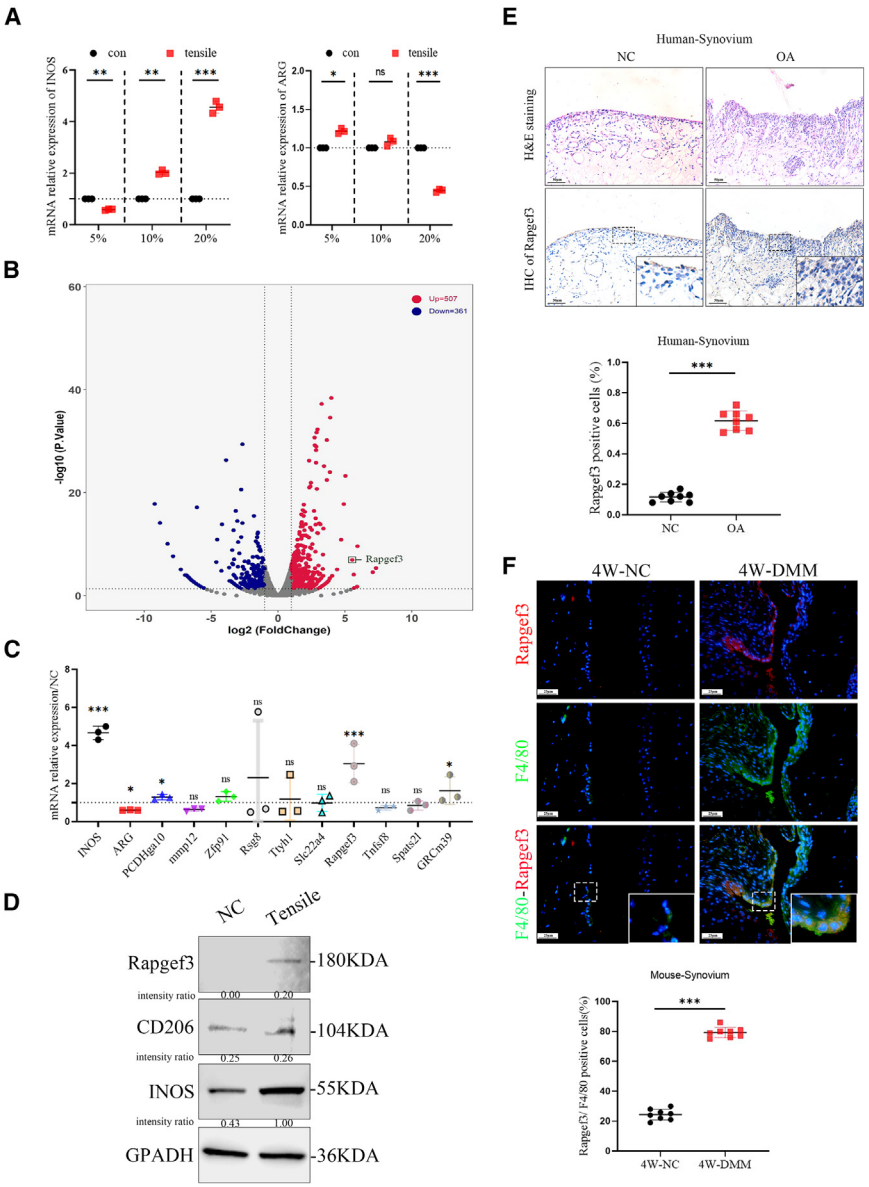

Figure 1. Increased macrophage Rapgef3 expression under excessive mechanical loading and in OA synovium

(A) Relative INOS and ARG mRNA expression in RAW246.7 cells treated with different elongation strain loads (5%, 10%, and 20%) for 24 h, $n = 3$ per group.

(B) Differentially expressed mRNA in RAW246.7 cells treated with normal and 20% elongation strain loading for 24 h.

(C) The mRNA expression levels of the top 10 genes that were differentially expressed in RAW246.7 cells treated with normal and 20% elongation strain loading for 24 h, $n = 3$ per group.

(D) Immunoblotting of GAPDH, INOS, CD206, and Rapgef3 of RAW264.7 cells treated with 20% elongation strain loading for 24 h. Full-length blots/gels are presented in Data S1 Original Western Blots −1.

(E) Hematoxylin and eosin (H&E) (upper) and immunohistochemistry (IHC) for Rapgef3 (middle) from human synovial tissues of patients with no history of patients with arthritis and OA. Scale bar: 50 μm. Description of Rapgef3 quantification in synovial tissues (lower), $n = 8$ per group.

(F) Immunofluorescence (IF) staining and quantification of Rapgef3 and F4/80 in knee synovium of 4-week sham operation mice and 4-week DMM mice, $n = 8$ per group. Scale bar: 25 μm.

$^{*}p < 0.05$, $^{**}p < 0.01$, $^{***}p < 0.001$, ns not significant. Data are shown as means ± SD. Statistical analysis was performed by unpaired t test (A, C, E, and F). The box area on the right is enlarged.

with Rapgef3-overexpression plasmid. The results showed that the different plasmid concentrations did not produce significant changes in MMP13, COL2, SOX9, or P21 in primary mouse chondrocytes (Figures 3B and 3C). These results indicated that Rapgef3 had no direct effect on chondrocytes. However, previous results showed that Rapgef3 enhanced macrophage pro-inflammatory. Therefore, we proposed that Rapgef3 affected chondrocytes by mediating macrophage reprogramming.

Rapgef3 indirectly causes chondrocyte metabolic disorders by regulating the pro-inflammatory response of macrophages

To confirm this hypothesis, supernatant of macrophage treated with lipopolysaccharide (LPS) or Rapgef3-overexpression plasmid for 72 h was collected and co-cultured with chondrocytes. Quantitative polymerase chain reaction and western blot showed that the culture supernatant of macrophages treated with LPS promoted MMP13 in primary chondrocytes and inhibited COL2 and SOX9. Similarly, the cultured supernatants of overexpressed Rapgef3 (OE-Rapgef3) macrophages also promoted MMP13 expression and inhibited COL2 and SOX9 in chondrocytes (Figures 4A, 4B, and S3A).

Furthermore, macrophage supernatant from the untreated group (NC), excessive mechanical loading-treated group (tensile), and excessive mechanical loading-treated group with Rapgef3 knockdown (tensile-siRapgef3) was collected for co-culture with chondrocytes. The MMP13 and P21 levels were upregulated, whereas COL2 and SOX9 were inhibited in chondrocytes treated with macrophage supernatant from the tensile group. Notably, these changes were reversed by knocking down macrophage Rapgef3 (Figures 4C, 4D, and S3B). Moreover, when tibial plateau cartilage explants from 3-week-old mice were cultured with OE-Rapgef3 macrophage supernatant for 5 days, significant proteoglycan loss was observed (Figures 4E and S3C). Rapgef3 knockdown in macrophages significantly alleviated proteoglycan loss in chondrocytes co-cultured with excessive mechanical loading-treated macrophage

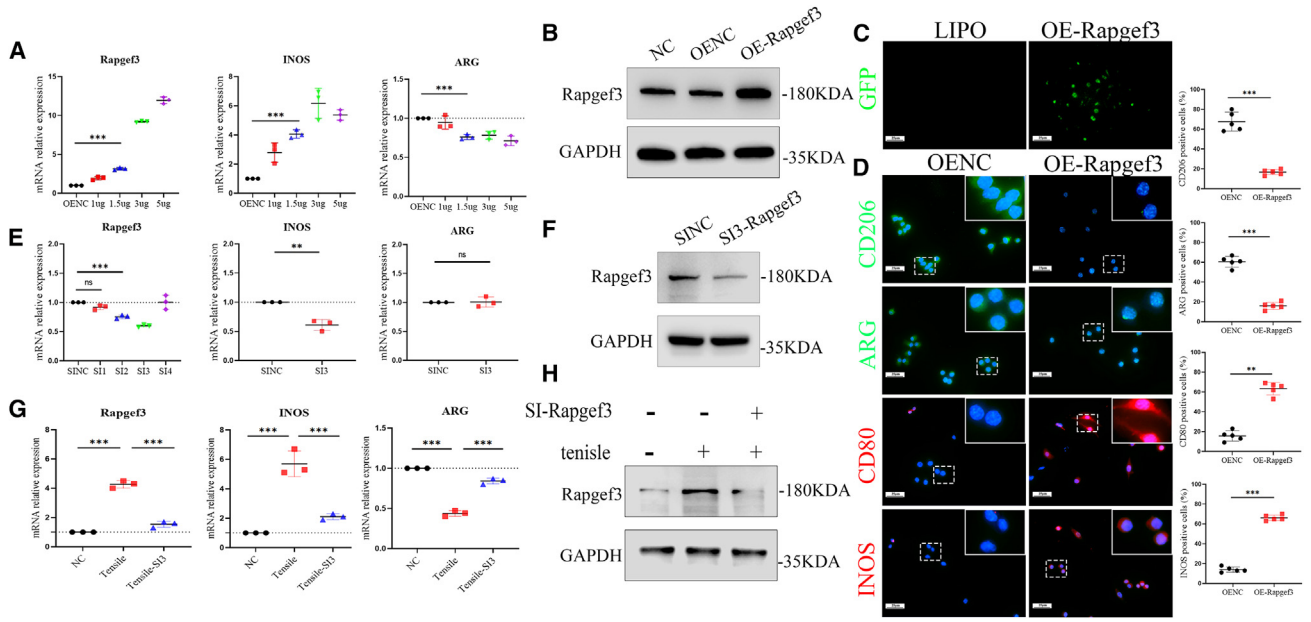

Figure 2. Rapgef3 enhances pro-inflammatory of macrophages and inhibition of Rapgef3 reduces pro-inflammatory

(A) Relative Rapgef3, INOS, and ARG mRNA expression levels in RAW246.7 cells transfected with Rapgef3 plasmid at different concentrations (1, 1.5, 3, and 5 μg/mL) for 48 h, $n = 3$ per group.

(B) Immunoblotting of GAPDH and Rapgef3 in RAW246.7 cells transfected with 3 μg/mL Rapgef3 plasmid and Rapgef3 control plasmid for 72 h. Full-length blots/gels are presented in Data S1 Original Western Blots −2.

(C) Cell immunofluorescence staining (Cell IF staining) of GTP (labels that overexpress the Rapgef3 plasmid) in RAW246.7 cells used lipo3000 and transfected with 3 μg/mL Rapgef3 plasmid for 72 h, $n = 5$ per group. Scale bar: 25 μm.

(D) Cell IF staining and quantification of CD206, ARG, CD80, and INOS in RAW246.7 cells transfected with 3 μg/mL Rapgef3 plasmid and Rapgef3 control plasmid for 72 h, $n = 5$ per group. Scale bar: 25 μm.

(E) Relative Rapgef3 mRNA expression levels in RAW264.7 cells transfected for 48 h were controlled with different SIRapgef3 (SI1, SI2, SI3, and SI4) or siRNA negative control (SINC). The relative INOS and ARG mRNA expression levels in RAW264.7 cells transfected with SI3 and SINC for 48 h were controlled, $n = 3$ per group.

(F) Treat with SI3 or SINC transfected into normal RAW264.7 cells. Immunoblotting for GAPDH and Rapgef3 in RAW264.7 cells. Full-length blots/gels are presented in Data S1 Original Western Blots −2.

(G) Relative Rapgef3, INOS, and ARG mRNA expression levels in RAW264.7 cells at 20% elongation strain load and transfected with/without SIRapgef3 at 20% elongation strain load for 24 h, $n = 3$ per group.

(H) Immunoblotting for GAPDH and Rapgef3 in RAW264.7 cells at 20% elongation strain load with/without SIRapgef3 transfection for 24 h. Full-length blots/gels are presented in Data S1 Original Western Blots −2.

$^{*}p < 0.05$, $^{**}p < 0.01$, $^{***}p < 0.001$, ns not significant. Data are shown as means ± SD. Statistical analysis was performed by unpaired t test (A, E, and G).

supernatants (Figures 4F and S3D). These results indicated that Rapgef3 had no direct effect on chondrocytes; rather, it indirectly damaged chondrocytes by mediating macrophage polarization.

Inhibition of Rapgef3 reverses synovitis and cartilage lesions in mice

To further determine the role of Rapgef3 in OA, RAW246.7 cells were transfected with a lentivirus (multiplicity of infection = 40 vgs/cell) carrying Rapgef3-siRNA, and Rapgef3 was knocked down in RAW246.4 cells (Figure S4A). Male 10-week-old C57 mice were intra-articularly injected with the lentivirus twice weekly after DMM surgery for 4 weeks. Compared to controls (DMM group), knocking down Rapgef3 reversed synovitis and cartilage lesions, characterized by decreased synovitis and Osteoarthritis Research Society International scores (Figures 5A–5F). Moreover, upregulated COL2 and SOX9 expression and reduced MMP13 expression were also observed in tibial cartilage on Rapgef3 knockdown (Figures 5G–5L). This suggested that reducing Rapgef3 rescued synovial inflammation and metabolic disorders of chondrocytes during OA development.

Rapgef3 promotes macrophage inflammatory by activating the p65/NF-κB pathway

We subsequently assessed how Rapgef3 induces pro-inflammatory macrophages. Earlier studies have shown that Rapgef3 activates the NF-κB pathway.[26] This pathway is a well-studied inflammatory pathway that is overactivated in OA, contributing to synovitis exacerbation, pro-inflammatory macrophage induction, and chondrocyte matrix degradation.[27–30]

At the cellular level, the results showed that Rapgef3 overexpression activated the p65/NF-κB pathway in macrophages compared with controls (Figure 6A). Treatment with a 0.5 Hz and 20% cyclic tensile strain load also activated the p65/NF-κB pathway in macrophages, and Rapgef3 knockdown inhibited

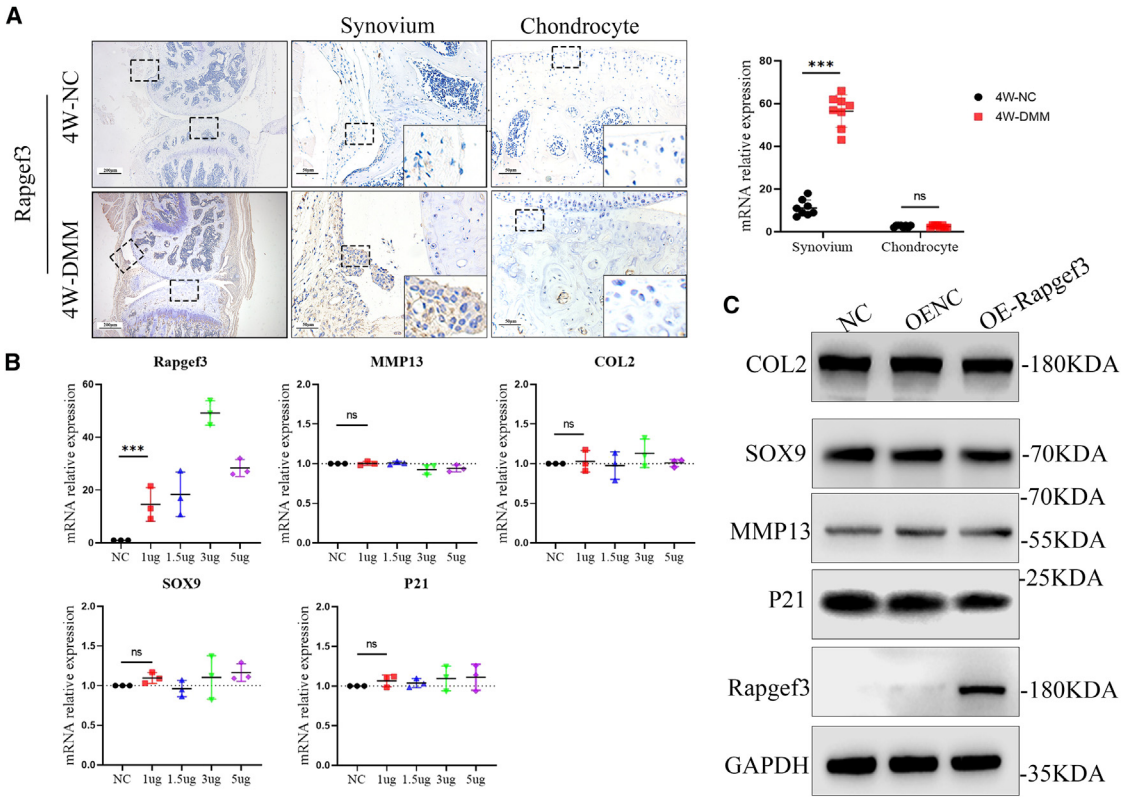

Figure 3. Rapgef3 has no direct effect on chondrocytes

(A) Immunohistochemistry (IHC) and quantification of Rapgef3 in knee synovium and knee cartilage of 4-week sham operation mice and 4-week DMM mice, $n = 8$ per group. Scale bar: 50 μm, 200 μm.

(B) Primary murine chondrocytes transfected with Rapgef3 plasmid at different concentrations (1, 1.5, 3, and 5 μg/mL) for 48 h, $n = 3$ per group.

(C) Immunoblotting for GAPDH, Rapgef3, MMP13, COL2, SOX9, and P21 in primary murine chondrocytes transfected with 3 μg/mL Rapgef3 plasmid or Rapgef3 control plasmid for 72 h. Full-length blots/gels are presented in Data S1 Original Western Blots −3.

*$p < 0.05$, **$p < 0.01$, ***$p < 0.001$, ns not significant. Data are shown as means ± SD. Statistical analysis was performed by unpaired t test (A and B). The box area on the right is enlarged.

p65 phosphorylation (Figure 6B). *In vivo*, knocking down Rapgef3 inhibited the p65/NF-κB pathway in synovial macrophages (Figure 6C). Therefore, we concluded that Rapgef3 in macrophages promoted inflammatory macrophages by activating the p65/NF-κB pathway, thereby exacerbating synovitis and cartilage degeneration and ultimately worsening OA.

DISCUSSION

In this study, we demonstrated for the first time, to our knowledge, that Rapgef3 plays a crucial role in mediating macrophage polarization and indirectly influencing chondrocyte synthesis catabolism during the pathogenesis and progression of OA. We observed a significant upregulation of Rapgef3 in synovial macrophages due to excessive mechanical loading, which subsequently affected macrophage polarization through NF-κB signaling. This exacerbates synovial inflammation and disrupts chondrocyte homeostasis during OA. Our findings highlight an important functional pathway involved in OA development and suggest that inhibiting intra-articular Rapgef3 could be a potential therapeutic approach for preventing and treating OA.

The role of excessive mechanical loading in the occurrence and development of OA is well established. Excessive mechanical loading in OA can stimulate chondrocytes to produce a significant amount of MMP13, leading to alterations in the extracellular matrix,[31] cause increased mitochondrial superoxide generation in chondrocytes,[32] and induce iron-dependent apoptosis and aging of chondrocytes.[33,34] These findings indicate that there is a strong correlation between excessive mechanical loading and OA severity. However, the regulatory mechanism underlying this relationship remains unclear. In our study, we found that the expression of mRNA in CD206/ARG1 increased slightly in the low load-exposed cells, which may suggest that tensile stress regulates macrophages mainly by affecting the expression of pro-inflammatory macrophages. Additionally, knockdown of Rapgef3 significantly inhibited pro-inflammation of macrophages induced by excessive mechanical loading. This inhibition indirectly affected chondrocyte anabolism. Similarly, lentivirus that knocks down Rapgef3 effectively reversed synovitis and articular cartilage destruction in mechanically loaded DMM-OA mice. These results indicate that Rapgef3 regulates the effects of excessive mechanical

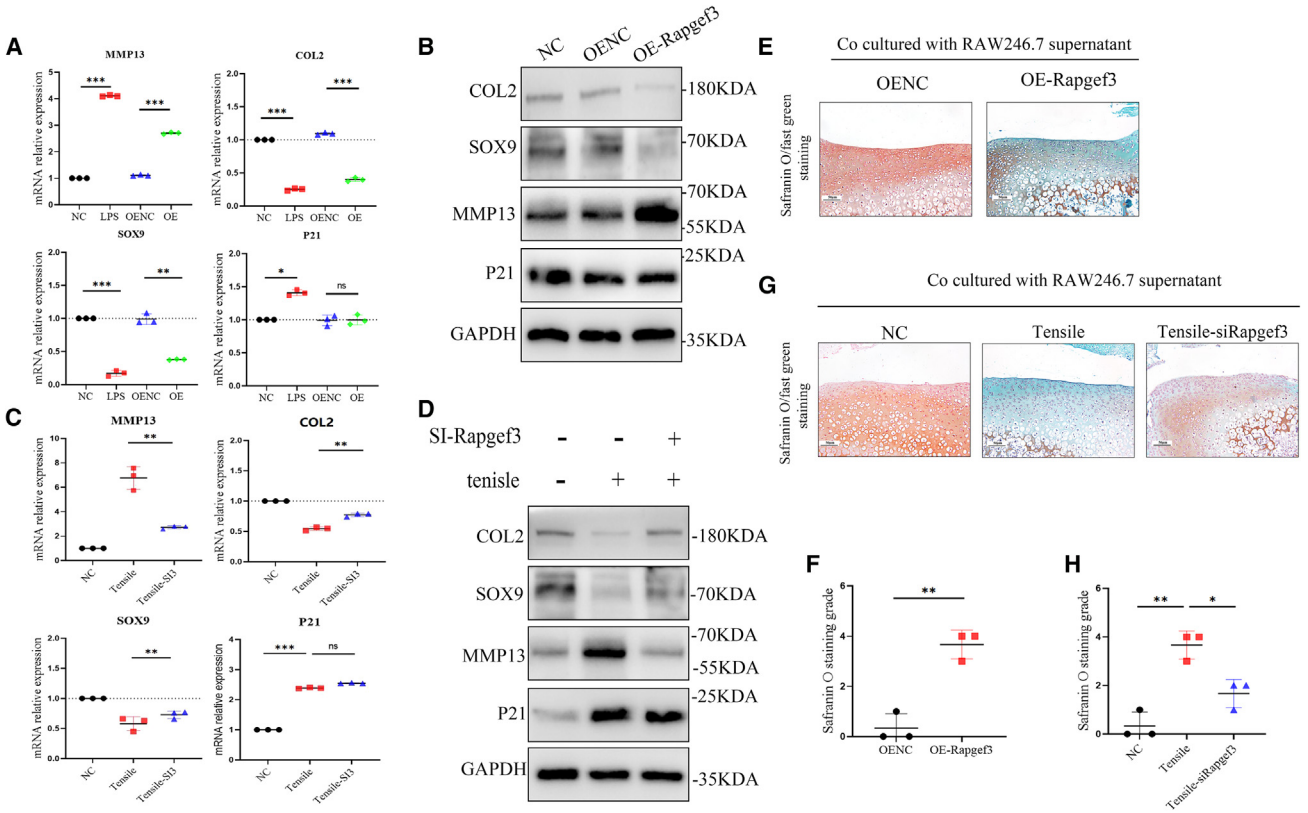

Figure 4. Rapgef3 indirectly causes chondrocyte metabolic disorders by regulating the pro-inflammatory response of macrophages

(A) Relative mRNA expression levels of MMP13, COL2, SOX9, and P21 in primary mouse chondrocytes co-cultured with the superserum of RAW264.7 for 48 h (RAW264.7 cells were treated with LPS or transfected with 3 μg/mL Rapgef3 plasmid for 48 h), $n = 3$ per group.

(B) Immunoblotting for MMP13, COL2, SOX9, and P21 in primary mouse chondrocytes co-cultured with the superserum of RAW264.7 for 48 h (RAW264.7 cells transfected with 3 μg/mL Rapgef3 plasmid or Rapgef3 control plasmid for 72 h), $n = 3$ per group. Full-length blots/gels are presented in Data S1 Original Western Blots −4.

(C and D) Relative mRNA expression levels and western blot of MMP13, COL2, SOX9, and P21 in primary mouse chondrocytes co-cultured with RAW264.7 superserum for 72 h (RAW264.7 cells treated with 20% elongation strain load with/without SIRapgef3 transfection for 24 h), $n = 3$ per group. Full-length blots/gels are presented in Data S1 Original Western Blots −4.

(E and F) Safranin O staining and grading of mouse tibial plateau cartilage explants co-cultured with RAW264.7 superserum for 5 days (RAW264.7 transfected with 3 μg/mL Rapgef3 plasmid or Rapgef3 control plasmid for 72 h), $n = 3$ per group. Scale bar: 25 μm.

(G and H) Safranin O staining and grading of mouse tibial plateau cartilage explants co-cultured with RAW264.7 superserum for 5 days (RAW264.7 treated with 20% elongation strain load with/without SIRapgef3 transfection for 24 h), $n = 3$ per group. Scale bar: 25 μm.

$^*p < 0.05$, $^{**}p < 0.01$, $^{***}p < 0.001$, ns not significant. Data are shown as means ± SD. Statistical analysis was performed by unpaired t test (A, C, F, and H).

loading on synovium and cartilage, potentially contributing to OA pathogenesis.

Recent evidence suggested that an imbalance in pro-inflammatory/anti-inflammatory macrophages played a critical role in OA-associated inflammation.[16] Pro-inflammatory macrophages, but not anti-inflammatory macrophages, accumulate in human and mouse OA synovial tissue.[35] We discovered that exogenous Rapgef3 enhances pro-inflammatory macrophages and affects the metabolic balance of chondrocytes, ultimately exacerbating OA.

There is currently no definite conclusion on the role of Rapgef3 in inflammation. Rapgef3 deletion led to reduced retinal vascular inflammation after retinal ischemia,[22] but it has also been reported that Rapgef3 deletion increased the retinal inflammatory pathway in mice.[36] These inconsistencies may be due to the fact that different cell types can exhibit different expression patterns and thus similar stimuli may produce opposite results. Our study found that in OA, administration of lentivirus that knocks down Rapgef3 effectively reversed synovitis and partially prevented cartilage destruction. Moreover, some studies have found that Rapgef3 activated the NF-κB pathway that is closely associated with macrophage polarization.[24] Our intervention experiments in macrophages and mouse joint synovial macrophages verified this. These results indicated that Rapgef3 was an important contributor to OA occurrence and development.

In conclusion, our findings demonstrate that excessive mechanical loading induces an upregulation of Rapgef3 expression in synovial macrophages. This increased Rapgef3 expression subsequently triggering the activation of the NF-κB pathway, leading to polarization and inflammation of synovial macrophages, ultimately exacerbating OA. Lentiviruses that knock down Rapgef3 can effectively reverse synovitis and chondrocyte degradation. Analyzing the interplay between Rapgef3,

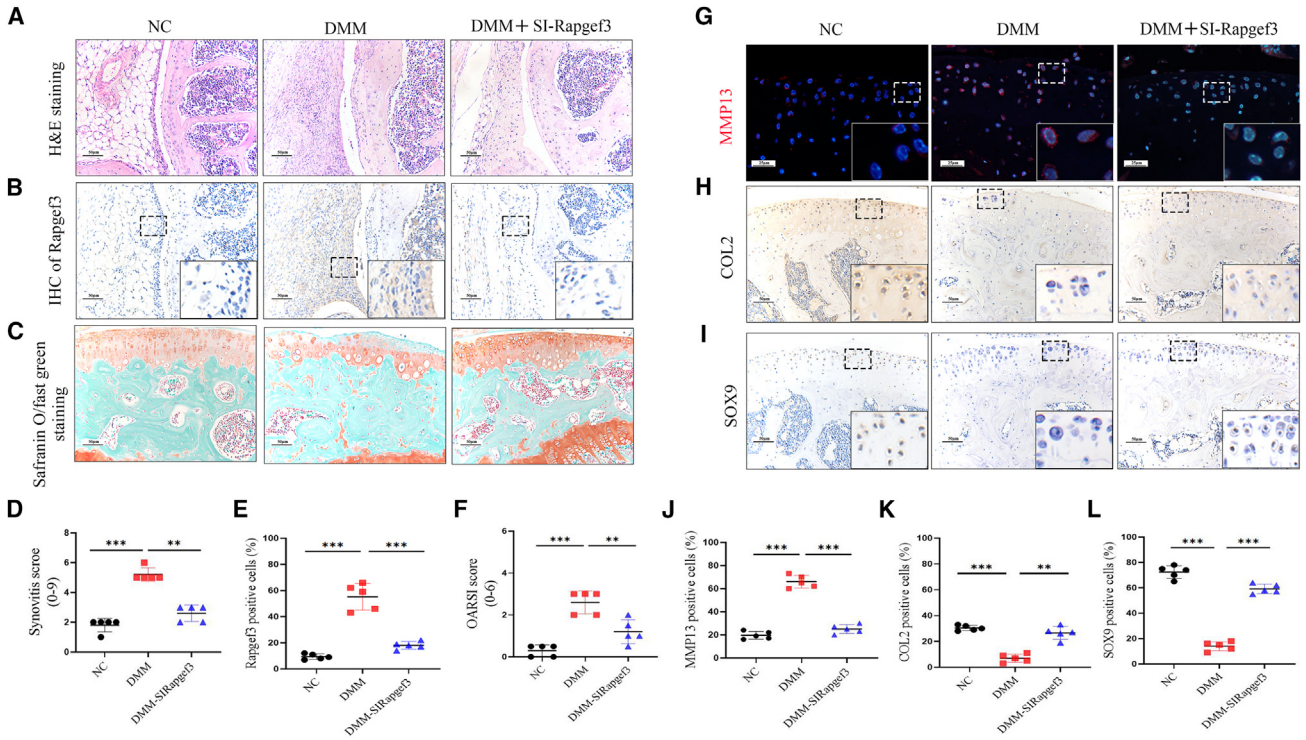

Figure 5. Inhibition of Rapgef3 reverses synovitis and cartilage lesions in mice

(A) H&E staining of knee synovial tissue from sham surgery and DMM mice treated for 4 weeks with a lentivirus vector that knocks down Rapgef3 (SI-Rapgef3). Scale bar: 50 μm.

(B) Immunohistochemical staining for Rapgef3 in knee synovial tissue from sham surgery and DMM mice treated for 4 weeks with a lentivirus vector that knocks down Rapgef3. Scale bar: 50 μm.

(C) Safranin O and Fast Green staining of knee cartilage from sham surgery and DMM mice treated for 4 weeks with a lentivirus vector that knocks down Rapgef3. Scale bar: 50 μm.

(D) Synovitis score of the joint described in (A), $n = 5$ per group.

(E) Quantification of Rapgef3 in articular synovium described in (B), $n = 5$ per group.

(F) Osteoarthritis Research Society International (OARSI) grades for the joints described in (C), $n = 5$ per group.

(G) Immunofluorescence staining for MMP13 in knee cartilage tissue from sham surgery and DMM mice treated with a carrier, Rapgef3 lentivirus, for 4 weeks. Scale bar: 25 μm.

(H) Immunohistochemical staining for COL2 in knee cartilage tissue from sham surgery and from DMM mice treated for 4 weeks with a lentivirus carrier that knocks down Rapgef3. Scale bar: 50 μm.

(I) Immunohistochemical staining for SOX9 in knee cartilage tissue from sham surgery and DMM mice treated for 4 weeks with a lentivirus carrier that knocks down Rapgef3. Scale bar: 50 μm.

(J) Quantification of MMP13 in articular cartilage described in (G), $n = 5$ per group.

(K) Quantification of COL2 in articular cartilage described in (H), $n = 5$ per group.

(L) Quantification of SOX9 in articular cartilage described in (I), $n = 5$ per group.

$^{*}p < 0.05$, $^{**}p < 0.01$, $^{***}p < 0.001$, ns not significant. Data are shown as means ± SD. Statistical analysis was performed by unpaired t test (D, E, F, J, K, and L). The box area on the right is enlarged.

macrophages, and chondrocytes offers a new approach for studying OA development. While clinical evidence supporting the inhibition of Rapgef3 in OA is currently lacking, modulating macrophage polarization may serve as a potential strategy to delay OA progression.

Limitations of the study

This study has its limitations and provides a research direction for the future. We found that culturing chondrocytes with supernatant from macrophages that were loaded with 0.5 Hz and 20% cyclic tensile strain affected the chondrocyte aging index (P21 increase), but culture of chondrocytes with supernatant from macrophages that overexpressed Rapgef3 had no effect on chondrocyte aging. Therefore, we hypothesized that chondrocyte aging may be regulated by other mediators. Despite these limitations, this study reports for the first time that synovitis induced by Rapgef3 under excessive mechanical loading further affects chondrocytes and aggravates OA.

RESOURCE AVAILABILITY

Lead contact

Further information and requests for resources and reagents should be directed to and will be fulfilled by the lead contact, Haiyan Zhang (zhhy0704@126.com).

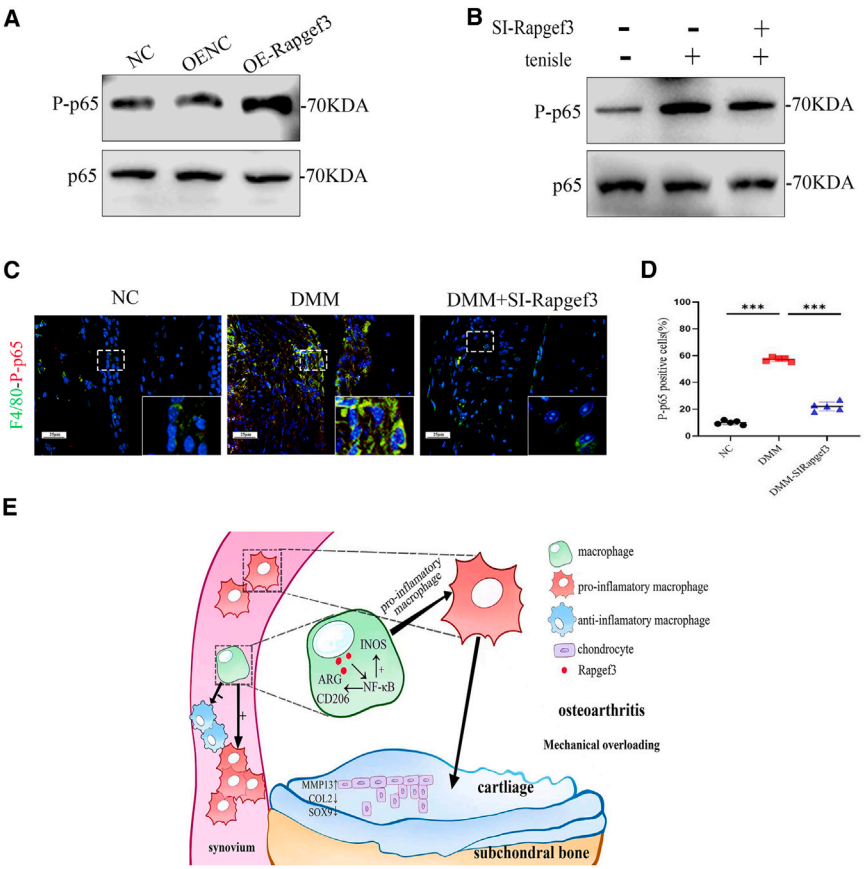

Figure 6. Rapgef3 promotes macrophage inflammatory by activating the p65/NF-κB pathway

(A) Immunoblotting of p65 and P-p65 in RAW246.7 cells transfected with 3 μg/mL Rapgef3 plasmid or Rapgef3 control plasmid for 72 h. Full-length blots/gels are presented in Data S1 Original Western Blots −6.

(B) Immunoblotting of p65 and P-p65 in RAW264.7 cells with 20% elongation strain load and transfected with/without SIRapgef3 for 24 h. Full-length blots/gels are presented in Data S1 Original Western Blots −6.

(C and D) Immunofluorescence staining and quantification of F4/80 and P-p65 in knee synovial tissue from sham surgery and DMM mice treated for 4 weeks with a lentivirus vector that knocks down Rapgef3, $n = 5$ per group. Scale bar: 25 μm.

(E) Model of Rapgef3 modulating synovial macrophage polarization and disrupting chondrocyte homeostasis during OA. Excessive mechanical loading can induce the increase of Rapgef3 in synovial macrophages, and the increased Rapgef3 promotes increased pro-inflammatory of synovial macrophages, and pro-inflammatory macrophages disrupt chondrocyte homeostasis and accelerate OA progression.

$^{*}p < 0.05$, $^{**}p < 0.01$, $^{***}p < 0.001$, ns not significant. Data are shown as means ± SD. Statistical analysis was performed by unpaired t test (C). The box area on the right is enlarged.

Materials availability

This study did not generate new unique reagents.

Data and code availability

- RNA-seq data have been deposited at the GEO database and are publicly available as of the date of publication. Accession numbers are listed in the key resources table. Original western blots are included in the supplemental information. All other data reported in this paper will be shared by the lead contact upon request.
- This paper does not report original code.
- Any additional information required to reanalyze the data reported in this paper is available from the lead contact upon request.

ACKNOWLEDGMENTS

This work was supported by the National Natural Science Foundation of China (82322044, 32171133), the National Key Research and Development Plan (2022YFC3601900 and 2022YFC3601902), and The Open Project of the Sixth Affiliated Hospital of Guangzhou Medical University (202301-302). The study was approved by the Ethics Committee of the Third Affiliated Hospital of Southern Medical University, and human samples were collected after obtaining informed consent. This study has been approved by the project "Research on Pathogenesis and Treatment of Osteoarthritis." All animal experiments were approved by the Southern Medical University Committee Animal Care and Use Committee (ethical approval number: SMUL2021014). Methods and results were conducted following the Declaration of Helsinki.

AUTHOR CONTRIBUTIONS

W.T., J.-b.Y., and R.-g.L. designed and performed experiments, analyzed the data, and wrote the manuscript; C.-y.W. and J.-l.H. performed part of the experiments and prepared the figures; J.-j.Z., L.-f.Y., and G.-m.L. conducted some of the experiments and extracted the cells; D.-z.C. revised the manuscript; H.-y.Z. provided funding acquisition; and L.-l.L., Y.-l.L., and H.-y.Z. provided project administration.

DECLARATION OF INTERESTS

The authors declare no competing interests.

STAR★METHODS

Detailed methods are provided in the online version of this paper and include the following:

- KEY RESOURCES TABLE
- EXPERIMENTAL MODEL AND STUDY PARTICIPANT DETAILS
  - Human samples
  - Animals and OA model
  - Cells
- METHOD DETAILS
  - Cartilage explants
  - Co-culture
  - Histological analysis
  - IHC/IF staining
  - Cell IF staining
  - Quantitative reverse transcription-polymerase chain reaction(RT-qPCR)
  - Western blot analysis (WB)
  - Plasmid transfection and siRNA transfection
- QUANTIFICATION AND STATISTICAL ANALYSIS

SUPPLEMENTAL INFORMATION

Supplemental information can be found online at https://doi.org/10.1016/j.isci.2025.112131.

Received: January 31, 2024
Revised: April 11, 2024
Accepted: February 26, 2025
Published: March 30, 2025

REFERENCES

1. Martel-Pelletier, J., Barr, A.J., Cicuttini, F.M., Conaghan, P.G., Cooper, C., Goldring, M.B., Goldring, S.R., Jones, G., Teichtahl, A.J., and Pelletier, J.P. (2016). Osteoarthritis. Nat. Rev. Dis. Primers *2*, 16072. https://doi.org/10.1038/nrdp.2016.72.
2. Prieto-Alhambra, D., Judge, A., Javaid, M.K., Cooper, C., Diez-Perez, A., and Arden, N.K. (2014). Incidence and risk factors for clinically diagnosed knee, hip and hand osteoarthritis: influences of age, gender and osteoarthritis affecting other joints. Ann. Rheum. Dis. *73*, 1659–1664. https://doi.org/10.1136/annrheumdis-2013-203355.
3. Ter Heegde, F., Luiz, A.P., Santana-Varela, S., Magnúsdóttir, R., Hopkinson, M., Chang, Y., Poulet, B., Fowkes, R.C., Wood, J.N., and Chenu, C. (2020). Osteoarthritis-related nociceptive behaviour following mechanical joint loading correlates with cartilage damage. Osteoarthr. Cartil. *28*, 383–395. https://doi.org/10.1016/j.joca.2019.12.004.
4. Reyes, C., Leyland, K.M., Peat, G., Cooper, C., Arden, N.K., and Prieto-Alhambra, D. (2016). Association Between Overweight and Obesity and Risk of Clinically Diagnosed Knee, Hip, and Hand Osteoarthritis: A Population-Based Cohort Study. Arthritis Rheumatol. *68*, 1869–1875. https://doi.org/10.1002/art.39707.
5. Miller, R.E., Scanzello, C.R., and Malfait, A.M. (2019). An emerging role for Toll-like receptors at the neuroimmune interface in osteoarthritis. Semin. Immunopathol. *41*, 583–594. https://doi.org/10.1007/s00281-019-00762-3.
6. Monteagudo, S., Cornelis, F.M.F., Aznar-Lopez, C., Yibmantasiri, P., Guns, L.A., Carmeliet, P., Cailotto, F., and Lories, R.J. (2017). DOT1L safeguards cartilage homeostasis and protects against osteoarthritis. Nat. Commun. *8*, 15889. https://doi.org/10.1038/ncomms15889.
7. Wang, S., Li, W., Zhang, P., Wang, Z., Ma, X., Liu, C., Vasilev, K., Zhang, L., Zhou, X., Liu, L., et al. (2022). Mechanical overloading induces GPX4-regulated chondrocyte ferroptosis in osteoarthritis via Piezo1 channel facilitated calcium influx. J. Adv. Res. *41*, 63–75. https://doi.org/10.1016/j.jare.2022.01.004.
8. Chang, S.H., Mori, D., Kobayashi, H., Mori, Y., Nakamoto, H., Okada, K., Taniguchi, Y., Sugita, S., Yano, F., Chung, U.I., et al. (2019). Excessive mechanical loading promotes osteoarthritis through the gremlin-1-NF-κB pathway. Nat. Commun. *10*, 1442. https://doi.org/10.1038/s41467-019-09491-5.
9. Cooke, M.E., Lawless, B.M., Jones, S.W., and Grover, L.M. (2018). Matrix degradation in osteoarthritis primes the superficial region of cartilage for mechanical damage. Acta Biomater. *78*, 320–328. https://doi.org/10.1016/j.actbio.2018.07.037.
10. Pierson, E., Cutler, D.M., Leskovec, J., Mullainathan, S., and Obermeyer, Z. (2021). An algorithmic approach to reducing unexplained pain disparities in underserved populations. Nat. Med. *27*, 136–140. https://doi.org/10.1038/s41591-020-01192-7.
11. Zhang, H., Shao, Y., Yao, Z., Liu, L., Zhang, H., Yin, J., Xie, H., Li, K., Lai, P., Zeng, H., et al. (2022). Mechanical overloading promotes chondrocyte senescence and osteoarthritis development through downregulating FBXW7. Ann. Rheum. Dis. *81*, 676–686. https://doi.org/10.1136/annrheumdis-2021-221513.
12. Robinson, W.H., Lepus, C.M., Wang, Q., Raghu, H., Mao, R., Lindstrom, T.M., and Sokolove, J. (2016). Low-grade inflammation as a key mediator of the pathogenesis of osteoarthritis. Nat. Rev. Rheumatol. *12*, 580–592. https://doi.org/10.1038/nrrheum.2016.136.
13. Sokolove, J., and Lepus, C.M. (2013). Role of inflammation in the pathogenesis of osteoarthritis: latest findings and interpretations. Ther. Adv. Musculoskelet. Dis. *5*, 77–94. https://doi.org/10.1177/1759720x12467868.
14. Zhang, H., Cai, D., and Bai, X. (2020). Macrophages regulate the progression of osteoarthritis. Osteoarthr. Cartil. *28*, 555–561. https://doi.org/10.1016/j.joca.2020.01.007.
15. Kapoor, M., Martel-Pelletier, J., Lajeunesse, D., Pelletier, J.P., and Fahmi, H. (2011). Role of proinflammatory cytokines in the pathophysiology of osteoarthritis. Nat. Rev. Rheumatol. *7*, 33–42. https://doi.org/10.1038/nrrheum.2010.196.
16. Liu, B., Zhang, M., Zhao, J., Zheng, M., and Yang, H. (2018). Imbalance of M1/M2 macrophages is linked to severity level of knee osteoarthritis. Exp. Ther. Med. *16*, 5009–5014. https://doi.org/10.3892/etm.2018.6852.
17. Yan, Y., Lu, A., Dou, Y., Zhang, Z., Wang, X.Y., Zhai, L., Ai, L.Y., Du, M.Z., Jiang, L.X., Zhu, Y.J., et al. (2023). Nanomedicines Reprogram Synovial Macrophages by Scavenging Nitric Oxide and Silencing CA9 in Progressive Osteoarthritis. Adv. Sci. *10*, e2207490. https://doi.org/10.1002/advs.202207490.
18. Zhang, H., Lin, C., Zeng, C., Wang, Z., Wang, H., Lu, J., Liu, X., Shao, Y., Zhao, C., Pan, J., et al. (2018). Synovial macrophage M1 polarisation exacerbates experimental osteoarthritis partially through R-spondin-2. Ann. Rheum. Dis. *77*, 1524–1534. https://doi.org/10.1136/annrheumdis-2018-213450.
19. Schmidt, M., Dekker, F.J., and Maarsingh, H. (2013). Exchange protein directly activated by cAMP (epac): a multidomain cAMP mediator in the regulation of diverse biological functions. Pharmacol. Rev. *65*, 670–709. https://doi.org/10.1124/pr.110.003707.
20. Kato, Y., Yokoyama, U., Yanai, C., Ishige, R., Kurotaki, D., Umemura, M., Fujita, T., Kubota, T., Okumura, S., Sata, M., et al. (2015). Epac1 Deficiency Attenuated Vascular Smooth Muscle Cell Migration and Neointimal Formation. Arterioscler. Thromb. Vasc. Biol. *35*, 2617–2625. https://doi.org/10.1161/atvbaha.115.306534.
21. Krishnan, A., Bhasker, A.I., Singh, M.K., Rodriguez, C.I., Pérez, E.C., Altameemi, S., Lares, M., Khan, H., Ndiaye, M., Ahmad, N., et al. (2022). EPAC Regulates Melanoma Growth by Stimulating mTORC1 Signaling and Loss of EPAC Signaling Dependence Correlates with Melanoma Progression. Mol. Cancer Res. *20*, 1548–1560. https://doi.org/10.1158/1541-7786.Mcr-22-0026.
22. Liu, W., Ha, Y., Xia, F., Zhu, S., Li, Y., Shi, S., Mei, F.C., Merkley, K., Vizzeri, G., Motamedi, M., et al. (2020). Neuronal Epac1 mediates retinal neurodegeneration in mouse models of ocular hypertension. J. Exp. Med. *217*, e20190930. https://doi.org/10.1084/jem.20190930.
23. Robichaux, W.G., and Cheng, X. (2018). Intracellular cAMP Sensor EPAC: Physiology, Pathophysiology, and Therapeutics Development. Physiol. Rev. *98*, 919–1053. https://doi.org/10.1152/physrev.00025.2017.
24. Wang, X., Luo, C., Cheng, X., and Lu, M. (2017). Lithium and an EPAC-specific inhibitor ESI-09 synergistically suppress pancreatic cancer cell proliferation and survival. Acta Biochim. Biophys. Sin. *49*, 573–580. https://doi.org/10.1093/abbs/gmx045.
25. Mediero, A., Perez-Aso, M., and Cronstein, B.N. (2014). Activation of EPAC1/2 is essential for osteoclast formation by modulating NFκB nuclear translocation and actin cytoskeleton rearrangements. FASEB J. *28*, 4901–4913. https://doi.org/10.1096/fj.14-255703.
26. Park, T.Y., Baik, E.J., and Lee, S.H. (2013). Prostaglandin E_2-induced intercellular adhesion molecule-1 expression is mediated by cAMP/Epac signalling modules in bEnd.3 brain endothelial cells. Br. J. Pharmacol. *169*, 604–618. https://doi.org/10.1111/bph.12103.
27. Sun, S.C. (2017). The non-canonical NF-κB pathway in immunity and inflammation. Nat. Rev. Immunol. *17*, 545–558. https://doi.org/10.1038/nri.2017.52.

28. Liu, H., Zhu, Y., Gao, Y., Qi, D., Zhao, L., Zhao, L., Liu, C., Tao, T., Zhou, C., Sun, X., et al. (2020). NR1D1 modulates synovial inflammation and bone destruction in rheumatoid arthritis. Cell Death Dis. *11*, 129. https://doi.org/10.1038/s41419-020-2314-6.

29. Yin, H., Zhang, X., Yang, P., Zhang, X., Peng, Y., Li, D., Yu, Y., Wu, Y., Wang, Y., Zhang, J., et al. (2021). RNA m6A methylation orchestrates cancer growth and metastasis via macrophage reprogramming. Nat. Commun. *12*, 1394. https://doi.org/10.1038/s41467-021-21514-8.

30. Cao, Y., Tang, S., Nie, X., Zhou, Z., Ruan, G., Han, W., Zhu, Z., and Ding, C. (2021). Decreased miR-214-3p activates NF-κB pathway and aggravates osteoarthritis progression. EBioMedicine *65*, 103283. https://doi.org/10.1016/j.ebiom.2021.103283.

31. Grillet, B., Pereira, R.V.S., Van Damme, J., Abu El-Asrar, A., Proost, P., and Opdenakker, G. (2023). Matrix metalloproteinases in arthritis: towards precision medicine. Nat. Rev. Rheumatol. *19*, 363–377. https://doi.org/10.1038/s41584-023-00966-w.

32. Liu, Y., Zhang, Z., Li, T., Xu, H., and Zhang, H. (2022). Senescence in osteoarthritis: from mechanism to potential treatment. Arthritis Res. Ther. *24*, 174. https://doi.org/10.1186/s13075-022-02859-x.

33. Yao, X., Sun, K., Yu, S., Luo, J., Guo, J., Lin, J., Wang, G., Guo, Z., Ye, Y., and Guo, F. (2021). Chondrocyte ferroptosis contribute to the progression of osteoarthritis. J. Orthop. Translat. *27*, 33–43. https://doi.org/10.1016/j.jot.2020.09.006.

34. Wang, F., Cai, F., Shi, R., Wang, X.H., and Wu, X.T. (2016). Aging and age related stresses: a senescence mechanism of intervertebral disc degeneration. Osteoarthr. Cartil. *24*, 398–408. https://doi.org/10.1016/j.joca.2015.09.019.

35. Zhou, D., Huang, C., Lin, Z., Zhan, S., Kong, L., Fang, C., and Li, J. (2014). Macrophage polarization and function with emphasis on the evolving roles of coordinated regulation of cellular signaling pathways. Cell. Signal. *26*, 192–197. https://doi.org/10.1016/j.cellsig.2013.11.004.

36. Jiang, Y., Liu, L., Curtiss, E., and Steinle, J.J. (2017). Epac1 Blocks NLRP3 Inflammasome to Reduce IL-1β in Retinal Endothelial Cells and Mouse Retinal Vasculature. Mediators Inflamm. *2017*, 2860956. https://doi.org/10.1155/2017/2860956.

37. Krenn, V., Morawietz, L., Burmester, G.R., Kinne, R.W., Mueller-Ladner, U., Muller, B., and Haupl, T. (2006). Synovitis score: discrimination between chronic low-grade and high-grade synovitis. Histopathology *49*, 358–364. https://doi.org/10.1111/j.1365-2559.2006.02508.x.

38. Glasson, S.S., Chambers, M.G., Van Den Berg, W.B., and Little, C.B. (2010). The OARSI histopathology initiative - recommendations for histological assessments of osteoarthritis in the mouse. Osteoarthr. Cartil. *18*, S17–S23. https://doi.org/10.1016/j.joca.2010.05.025.

39. Ekenstedt, K.J., Sonntag, W.E., Loeser, R.F., Lindgren, B.R., and Carlson, C.S. (2006). Effects of chronic growth hormone and insulin-like growth factor 1 deficiency on osteoarthritis severity in rat knee joints. Arthritis Rheum. *54*, 3850–3858. https://doi.org/10.1002/art.22254.

40. Evellin, S., Nolte, J., Tysack, K., vom Dorp, F., Thiel, M., Weernink, P.A.O., Jakobs, K.H., Webb, E.J., Lomasney, J.W., and Schmidt, M. (2002). Stimulation of phospholipase C-epsilon by the M3 muscarinic acetylcholine receptor mediated by cyclic AMP and the GTPase Rap2B. J. Biol. Chem. *277*, 16805–16813. https://doi.org/10.1074/jbc.M112024200.

STAR★METHODS

KEY RESOURCES TABLE

REAGENT or RESOURCE	SOURCE	IDENTIFIER
Antibodies		
Rabbit Rapgef3	Abclonal	Cat#A4149; RRID: AB_2863197
Rabbit INOS	Immunoway	Cat# YT3169; RRID: N/A
Rabbit CD80	Abcam	Cat#ab254579; RRID: AB_2943070
Rabbit CD206	Abcam	Cat#ab64693; RRID: AB_1523910
Rabbit ARG1	Abcam	Cat# ab315110; RRID: AB_3096381
Rabbit MMP13	Affinity Biosciences	Cat#AF5355; RRID: AB_2837840
Rabbit COL2	Abcam	Cat# ab34712; RRID: AB_731688
Rabbit SOX9	Abclonal	Cat#A19710; RRID: AB_2862748
Rabbit P21	Abcam	Cat#ab109199; RRID: AB_10861551
Rabbit GADPH	Abcam	Cat#ab181603; RRID: AB_2687666
Mouse F4/80	Santa Cruz	Cat# sc-377009; RRID: AB_2927461
Rabbit P65	CST	Cat# C8242; RRID: N/A
Rabbit p-P65	CST	Cat#C3033; RRID: N/A
Mouse Alexa Fluor 488	Life Technologies	Cat#A-21202; RRID: AB_141607
Rabbit Alexa Fluor 594	Life Technologies	Cat#A-11012; RRID: AB_2534079
Deposited data		
GSE280230	GEO	https://www.ncbi.nlm.nih.gov/geo/query/acc.cgi?acc=GSE280230; GSE280230
Chemicals, peptides, and recombinant proteins		
PBS powder	Boster	AR0186
TBS powder	Boster	AR0187
Neutral gum	Biosharp Life Sciences	BL704A
Goat serum	Gibco	R37624
Collagenase II	Biosharp Life Sciences	BS164
RIPA lysis buffer	Boster	AR0102
Protease inhibitors Boster	Boster	AR1182
Phosphatase inhibitors Boster	Boster	AR1183
DAPI reagent Boster	Boster	AR1176
4% polyformaldehyde	Biosharp Life Sciences	BL539A
RIPA lysis buffer	Boster	AR0102
ECL developer	**FUDE BIO**	FD8000
Fetal bovine serum	Corning	35-081-CV
DMEM basic medium	Corning	10-092-CVRC
1640 basic medium	Corning	10-040-CVRC
Eosin dye	Sigma	15086-94-9
Hematoxylin dye	Sigma	517-28-2
Penicillin-streptomycin double resistance	Hyclone	SV30010
DNA transfection reagent -LipoFiter	Thermo Fisher Scientific	L3000075
Universal antibody diluent	Biosharp Life Sciences	BL1060A
Safranin O	Stain Solution Solarbio Life Sciences	G1067
Toluidine Blue	Stain Solution Solarbio Life Sciences	G3660
Universal antibody diluent	Abcam	ab79995

(*Continued on next page*)

Continued

REAGENT or RESOURCE	SOURCE	IDENTIFIER
Experimental models: Cell lines		
RAW246.7	Pricella	CL-0190
Experimental models: Organisms/strains		
C57BL/6J mouse	GemPharmatech	Strain NO.N000013
Oligonucleotides		
GAPDH Forward:AGGTCGGTGTGAACGGATTTG Reverse:TGTAGACCATGTAGTTGAGGTCA	TsingkeBiotechnologyCo.,Ltd.	N/A
Rapgef3 Forward:AGCTGATCCATTATGTACTGGGC Reverse:TGTAGACCATGTAGTTGAGGTCA	TsingkeBiotechnologyCo.,Ltd.	N/A
IONS Forward:GTTCTCAGCCCAACAATACAAGA Reverse:GTGGACGGGTCGATGTCAC	TsingkeBiotechnologyCo.,Ltd.	N/A
ARG Forward:GCTTCCCAGGAGGTGTAGATG Reverse:ATGTCGGTCGATTTGGTGAGA	TsingkeBiotechnologyCo.,Ltd.	N/A
Pcdhga10 Forward:AAATGTCGCCCCAGGAATG Reverse:GCTCTGAACGACTAGGGAGAA	TsingkeBiotechnologyCo.,Ltd.	N/A
MMP12 Forward:GAGTCCAGCCACCAACATTAC Reverse:GCGAAGTGGGTCAAAGACAG	TsingkeBiotechnologyCo.,Ltd.	N/A
Zfp91 Forward:GACCTCTATCTCTCGCCTTCG Reverse:AAGGAGCCAGTCTTGGACCTA	TsingkeBiotechnologyCo.,Ltd.	N/A
Rgs8 Forward:GCAGGAACAAAGGCATGAGGA Reverse:TGCTTCTTCCGTGGAGAGTCT	TsingkeBiotechnologyCo.,Ltd.	N/A
Ttyh1 Forward:CCGCGACCAAGAGTACCAG Reverse:GAAGCGGATGAGGTAGACAGC	TsingkeBiotechnologyCo.,Ltd.	N/A
Slc22a4 Forward:CGTGACAGAGTGGAATCTGGT Reverse:GAGAACGCCTACGAAGAACAG	TsingkeBiotechnologyCo.,Ltd.	N/A
Tnfsf8 Forward:GCAGCTACTTCTACCTCAGCA Reverse:GCCATCTTCGTTCCATGACAGT	TsingkeBiotechnologyCo.,Ltd.	N/A
Spats2l Forward:GCTGAACTCAACACTCATGTGA Reverse:GCTGAACTCAACACTCATGTGA	TsingkeBiotechnology Co.,Ltd.	N/A
GRCm39 Forward:AGAGGATGTACGGCTGTGAC Reverse:CACCTGCGTCGAGTGATCTG	TsingkeBiotechnologyCo.,Ltd.	N/A
MMP13 Forward:CTTCTTCTTGTTGAGCTGGACTC Reverse:CTGTGGAGGTCACTGTAGACT	TsingkeBiotechnologyCo.,Ltd.	N/A
COL2 Forward:CTTAGGACAGAGAGAGAAGG Reverse:ACTCTGGGTGGCAGAGTTTC	TsingkeBiotechnologyCo.,Ltd.	N/A

(*Continued on next page*)

Continued

REAGENT or RESOURCE	SOURCE	IDENTIFIER
SOX9 Forward:GAGCCGGATCTGAAGAGGGA Reverse:GCTTGACGTGTGGCTTGTTC	TsingkeBiotechnologyCo.,Ltd.	N/A
P21 Forward:CCTGGTGATGTCCGACCTG Reverse:CCATGAGCGCATCGCAATC	TsingkeBiotechnologyCo.,Ltd.	N/A
CD80 Forward:ACCCCCAACATA ACTGAGTCT Reverse:TTCCAACCAAGAGAAGCGAGG	TsingkeBiotechnologyCo.,Ltd.	N/A
CD206 Forward:CTCTGTTCAGCTATTGGACGC Reverse:CTCTGTTCAGCTATTGGACGC	TsingkeBiotechnologyCo.,Ltd.	N/A
Si-Rapgef3-1 Forward:GCUCUUACCAGCUAGUGUU Reverse:AACACUAGCUGGUAAGAGC	TsingkeBiotechnology Co.,Ltd.	N/A
Si-Rapgef3-2 Forward:GAGAUGCCCGACUUAGCAA Reverse:UUGCUAAGUCGGGCAUCUC	TsingkeBiotechnologyCo.,Ltd.	N/A
Si-Rapgef3-3 Forward:GCAGGAACUGUGUUGUUCA Reverse:UGAACAACACAGUUCCUGC	TsingkeBiotechnologyCo.,Ltd.	N/A
Si-Rapgef3-4 Forward:CUACUCAGGAAGUUCAUCA Reverse:UGAUGAACUUCCUGAGUAG	TsingkeBiotechnologyCo.,Ltd.	N/A
Software and algorithms		
ImageJ Version 1.53	National Institutes of Health	https://www.nih.gov/
GraphPad Prism Version 8	GraphPad Software	https://www.graphpad.com/
Adobe Photoshop 2022	Adobe	https://www.downkuai.com/soft/148842.html

EXPERIMENTAL MODEL AND STUDY PARTICIPANT DETAILS

Human samples

The source of human samples in this paper was approved by the Ethics Committee of the third affiliated Hospital of Southern Medical University and carried out with the informed consent of patients. Eight of the samples were taken from normal synovium of road traffic accident patients with no history of arthritis, whereas the other eight were taken from OA synovium of total knee arthroplasty patients, which served as control and OA group respectively. All the patients were treated in the third affiliated Hospital of Southern Medical University, and the sample collection was completed by the same person. Detailed information about the participants is provided in Table S1.

Animals and OA model

All animals were purchased from the Experimental Animal Center of Southern Medical University (Guangzhou, China). All animal experiments are approved by the Animal Care and Use Committee of the Southern Medical University Committee and are conducted in accordance with the regulations of the Committee. The importation, transportation and captivity of the mice were performed according to the recommendations of "Use of non-human primates in research". All mice are maintained according to institutional animal care and use guidelines. Before the experiment, all animals were randomly assigned to three groups (n=5), and 10-week-old male C57/BL6 mice were subjected to destabilization of the medial meniscus (DMM) surgery on the right knee to induce OA model. The mice were anesthetized with pentobarbital by intraperitoneal injection prior to surgery. The NC group of mice was sham operation group. Following surgery, in DMM group, 5μg/5μL/week lentivirus (TsingKe, BeiJing,China) with nonsense sequence was injected into the right knee cavity. In the treatment group,Rapgef3-knockout siRNA lentiviral vector (TsingKe, BeiJing,China) was injected 5μg/5μL/ week into the right knee cavity (DMM+SI-Rapgef3). The mice were euthanized 4 weeks after operation, and the specimens of right knee joint were collected. The Southern Medical University Animal Care and Use Committee approved all procedures involving mice.

Cells

Primary mouse chondrocytes were derived from the tibial plateau of 5-7 day-old C57/BL6 mice and cultured in Dulbecco modified Eagle's medium F12 (DMEM:F12) (Gibco, Carlsbad, CA,USA) containing 20% fetal bovine serum (Gibco) and 1% penicillin-streptomycin at 37°C and 5%CO2. Mouse macrophage-like RAW246.7 cells (Pricella, CL-0190) in DMEM growth maintained at 10% fetal bovine serum. Lipofectamine 3000 (Thermo Fisher Scientific, Waltham, MA, USA) was used for plasmid transfection.The RNA of the primary mouse chondrocytes transfected by Rapgef3 overexpression plasmid (1μg/ml, 1.5μg/ml, 3μg/ml, 5μg/ml) was collected 48 hours after transfection (TsingKe, BeiJing, China),Proteins of primary mouse chondrocytes transfected by Rapgef3 overexpression plasmid (3μg/ml) (TsingKe, BeiJing, China) were obtained at 72 h. The RNA of RAW246.7 cells transfected by Rapgef3 overexpression plasmid (1μg/ml, 1.5μg/ml, 3μg/ml, 5μg/ml) (TsingKe, BeiJing, China) or Rapgef3-siRNA (TsingKe, BeiJing, China) was collected 48 hours after transfection. Proteins of RAW246.7 cells transfected with Rapgef3 overexpression plasmid (3μg/ml) or Rapgef3-SiRNA were obtained 72 hours after transfection. Regarding excessive mechanical loading, we applied the method validated in our research group's previous studies[40]. In brief, RAW246.7 cells of 60%–70% density were inoculated onto a stretchable plate of fibrin-coated six-pore cells. A excessive mechanical loading cell model was induced in a 5%CO2 incubator by applying a cyclic tensile strain of 20% elongation for 24h using the FLEXCELL-5000 mechanical tensile system. Control cells were inoculated on the same plate and cultured without cyclic load-tensile strain. Primary bone marrow-derived macrophages were isolated from the bone marrow of 6-8-week-old C57 mice. The cells were inoculated in a six-hole petri dish (Corning, New York, USA) and cultured in modified Eagle's medium containing 37°C, 5% carbon dioxide, 10% fetal bovine serum, 100U/mL penicillin and 100mg/mL streptomycin .The culture medium was changed every 3 days. Mouse macrophage colony stimulating factor (RockyHill) was used to induce differentiation for 7 days at a concentration of 50ng/mL. Following incubation with M-CSF, the cells differentiated into resting BMDM.

METHOD DETAILS

Cartilage explants

Tibial plateau explants were isolated from 3-week-old male C57 mice after euthanasia. The tibial platform was separated using eye scissors at the position of the growth plate under the tibial platform, and other soft tissues such as synovium and muscle were removed under the microscope.Before treatment, the explants were cultured in DMEM/F12 containing 20% fetal bovine serum in a 96-well plate for 3 days (changing the medium every day). After 3 days, the activity of the explants was judged according to the color change of the replaced medium. Then the explants were treated with 72-hour cell supernatant of RAW246.7 cells with transfected plasmids OENC or OE-Rapgef3 and 24-hour cell supernatant of RAW246.7 cells transfected with NC, 20% stretch, or 20% stretch with Rapgef3-siRNA, respectively, for 5 days (changing the medium daily).

Co-culture

RAW246.7 cells were treated with plasmid OENC or OE-Rapgef3 for 72 hours, and the supernatant was collected. RAW246.7 cells were subjected to NC, 20% stretch or 20% stretch after transfection with lentivirus Rapgef3-siRNA for 24 hours, and the supernatant was collected.This supernatant was co-cultured with primary chondrocytes in 6-well plates (1mL supernatant and 1mL DMEM/F12 containing 20% fetal bovine serum) for 72 hours. In addition, the supernatant and tibia-plateau explants were co-cultured in 96-well plates (125μL supernatant and 125μL DMEM/F12 containing 20% fetal bovine serum) for 5 days.

Histological analysis

The knee joint was fixed with 4% paraformaldehyde for 24 hours, decalcified in 10% EDTA (pH=7.4) at 37°C for 21 days, and embedded in paraffin wax.Slices of 4 μm were used for hematoxylin and eosin (H&E) staining and Safranine O (Saf-O)/Fast green staining.The severity of synovitis was assessed by two blind observers on the basis of increased cell layers in the resident synovitis lining (1-3), resident cell density (1-3), and inflammatory infiltration (1-3), and the sum of the three scores (maximum site score 9) was calculated, with a sum of 0 or 1 for no synovitis, a sum of 2-4 for mild synovitis, and a sum of 5-9 for severe synovitis.[37] The Saf-O/Fast green stained sections were assigned grades 0-6 by two blind observers to grade cartilage degradation based on the developed OARSI scoring system[38]:0, normal cartilage; 0.5, Saf-O was slightly lost and no structural changes occurred; 1, cartilage surface fibrosis without loss of cartilage area; 2. vertical cracks or defects on the surface of cartilage (hyaline cartilage); 3-6, the cartilage is vertically cracked or eroded to the deepest part of the cartilage < 25% (grade 3), 25-50% (grade 4), 50-75% (grade 5) and >75% (grade 6). Saf-O/Fast green stained sections of cartilage explants were graded by two blind observers based on the area of dye loss using a modified 6-point scale using a previously published system: 0, normal explants; 1-3, affected the graft cartilage depth ≤ 1/2 and affected the platform ≤ 1/3(grade 1), 1/3-1/2 (grade 2), > 1/2 (grade 3) staining loss, respectively; 4-6, loss of staining with cartilage depth > 1/2 and involved platforms ≤ 1/3(grade 4), 1/3-1/2 (grade 5), > 1/2 (grade 6).[39]

IHC/IF staining

For the preparation of 4 μm by the above method, the slide was dewaxed, rehydrated, and washed in PBS three times for 5 minutes each time. Antigen repair was performed by heating the slices in a water bath at 60°C and overnight in Tris/EDTA (pH=9.0). They were subsequently returned to room temperature and washed in PBS.

For immunohistochemical staining (IHC), 3% hydrogen peroxide was added and left for 10 minutes to inactivate endogenous peroxidase activity. After washing with PBS, it was closed with 1% goat serum (Solarbio, Beijing, China) at 37°C for 1 h and incubated with primary antibody at 4°C for 12 h. After washing with PBS, the sections were incubated with species-matched horseradish peroxidase-conjugated secondary antibodies (J Jackson ImmunoResearch Laboratories, West Grove,PA, USA) at room temperature for 1 hour, with 3, 3-diaminobenzidine (DAB) subsequently used to observe the chromogen, and hematoxylin for counterstaining and finally sealed with neutral resin.

For immunofluorescence staining (IF), a secondary antibody conjugated with Alexa Fluor 488 or Alexa Fluor 594 (Life Technologies, Carlsbad, CA,USA) was added and incubated at room temperature in the dark for 1 hour. IF sections were treated and sealed with a 4, 6-diaminidine 2-phenylindole (DAPI; Thermo Fisher Scientific, Waltham, MA, USA) staining solution.

The following primary antibodies were used: rabbit anti-Rapgef3 (1:200 for IHC,1:300 for IF; Abclonal, Woburn, MA, USA, A4149), rabbit anti-MMP13 (IF 1:500; Affinity Biosciences, AF 5355), rabbit COL2 resistance (IHC 1:200; Abcam, ab 34712), rabbit anti-SOX9 (IHC 1:200, Abclonal, A19170), rabbit anti-P-P65 (IF 1:50; CST, Danvers, MA, USA, 3033), mouse anti-F4/80 (IF 1:50; Santa Cruz, sc-377009).

Cell IF staining

The processed RAW246.7 cells and BMDMs were treated with 4% paraformaldehyde to 15min, then then blocked the cells with 1% sheep serum at 37°C for 30 minutes, and placed with the primary culture antibodys (in 1% BSA, 0.1% Triton X-100) at 4°C for 12 hours. Fluor 594 or Alexa Fluor 488 at room temperature for 1 hour in dark and the nuclei were labeled with DAPI. The following primary antibodies were used: rabbit antibody Rapgef3(1; 100; Abclonal, Woburn, MA, USA, A4149), rabbit anti-INOS (1:100; Immunoway, Plano, TX, USA, YT3169), rabbit anti-CD80 (1:100; Abcam,ab254579), rabbit anti-CD206 (1:100; Abcam,ab64693), rabbit anti-ARG (1:100; Abcam,ab315110).

Quantitative reverse transcription-polymerase chain reaction(RT-qPCR)

Total RNA was isolated from primary mouse chondrocytes and RAW246.7 cells using TRIzol reagent (Takara Bio Inc, Shiga, Japan). Total RNA was purified with genomic (gDNA) remover, and 5× HiScript II qRT Super-Mix II (Vazyme Biotech, Nanjing, China) reverse transcription cDNA. PCR was performed using 10 μL 2× ChamQ SYBR qPCR Master Mix (Vazyme) on a light cycler (Roche, Basel, Switzerland) with the primers listed in key resources table.

Western blot analysis (WB)

RAW264.7 cells and primary chondrocytes cultured in six-well petri dish were lysed with 200μL radioimmunoprecipitation assay (RIPA) buffer containing both phosphatase and protease inhibitors (Bey-time Institute of Biotechnology, Jiangsu, China). Cell lysates were analyzed by sodium dodecyl sulfatepolyacrylamide gel electrophoresis and transferred to a nitrocellulose membrane (Bio-Rad Corp, Hercules, CA, USA). After incubating with 5% buttermilk in 50mM Tris-buffered saline (TBS) containing 0.1% Tween-20 (TBST) (pH 7.4) at room temperature for 1 hour, the membrane was further incubated with primary antibody diluted with 5%BSA TBST at 4° C for 12 hours. The membrane was washed with TBST three times (5 minutes each time) and incubated with the secondary antibody (diluted with TBST at 1:4000) at room temperature for 1 hour.The target protein bands were visualized by FDBIO-DURA ECL (FDbio science, Hangzhou, China). The following primary antibodies for WB were used: rabbit antibody Rapgef3(1; 2000; Abclonal, Woburn, MA, USA, A4149), rabbit anti-INOS (1:1,000; Immunoway, Plano, TX, USA, YT3169), rabbit anti-CD206 (1:1, 000; Abcam, ab64693), rabbit anti-GAPDH (1:10,000; Abcam, ab181603), rabbit resistance to MMP13(1:2000; Affinity Biosciences, AF5355), rabbit COL2 resistance (1:1000; Abcam, ab34712), rabbit anti-SOX9 (1:2000; Abclonal, A19170) for rabbit resistance to P65(1; 1000; CST,8242), rabbit resistance to p-P65 (1:1000; CST, Danvers, MA, USA,3033).species-matched horseradish peroxidase-conjugated secondary antibodies (Jackson ImmunoResearch Laboratories, West Grove, PA, USA).

Plasmid transfection and siRNA transfection

According to the manufacturer's plan, lipofectamine 3000 (2.5 μL/mL) (Thermo Fisher Scientific) was used to compare the 3 μg/mL Rapgef3 plasmid with the plasmid (TsingKe) were transfected into RAW264.7 cells and primary mouse chondrocytes and medium for 48 hours. A total of 50 nanomol siRapgef3 or siRapgef3 with C0535 LipoRNAi^{TM} (2.5 μL/mL) (TsingKe) were transfected into normal RAW 264.7 cells and RAW 264.7 cells with cyclic tensile strain of 20% elongation for 24 h. The cells are then treated with Trizol for RNA analysis or RIPA for western blot analysis as described above.

The sequence of Rapgef3 overexpression plasmid was obtained from literature reading.[40] Detailed information about the participants is provided in key resources table.

QUANTIFICATION AND STATISTICAL ANALYSIS

All experiments were conducted in two or three copies and were observed by independent observers. Adobe Photoshop 2021 was used for image processing, GraphPad Prism 8.0.2 was used for graph generation and statistical analysis. The specific statistical analysis of all results is illustrated in the digital legend. The RNA sequencing data of RAW264.7 cells treated with 0.5 Hz and 0% cyclic tensile strain and 0.5 Hz and 20% cyclic tensile strain were uploaded to dataset GSE280230. Between-group comparisons of normally distributed data were performed using a Student's t-test. All statistical tests were two-tailed.

Statistical significance is denoted as follows: *$p < 0.05$; **$p < 0.01$; ***$p < 0.001$; ****$p < 0.0001$; ns, $p > 0.05$. The statistical details of all experiments can be found in the legend.